SECURITY

AD-A209 373 ITATION PAGE

Form Approved
OMB No. 0704-0188

1a. REP((	1b. RESTRICTIVE MARKINGS N/A
2a. SECU ... AUTHORITY N/A	3. DISTRIBUTION/AVAILABILITY OF REPORT Distribution Unlimited
2b. DECLASSIFICATION/DOWNGRADING SCHEDULE N/A	

4. PERFORMING ORGANIZATION REPORT NUMBER(S) N/A	5. MONITORING ORGANIZATION REPORT NUMBER(S) N/A

6a. NAME OF PERFORMING ORGANIZATION Stanford University	6b. OFFICE SYMBOL (If applicable) N/A	7a. NAME OF MONITORING ORGANIZATION Office of Naval Research
6c. ADDRESS (City, State, and ZIP Code) Sponsored Projects Office Jordan Quad/Birch/125 Panama St. Stanford, CA 94305		7b. ADDRESS (City, State, and ZIP Code) 800 N. Quincy St. Arlington, VA 22217-5000

8a. NAME OF FUNDING/SPONSORING ORGANIZATION Office of Naval Research	8b. OFFICE SYMBOL (If applicable) ONR	9. PROCUREMENT INSTRUMENT IDENTIFICATION NUMBER N000-14-86-K-0388

| 8c. ADDRESS (City, State, and ZIP Code) 800 N. Quincy St. Arlington, VA 22217-5000 | 10. SOURCE OF FUNDING NUMBERS |

PROGRAM ELEMENT NO	PROJECT NO.	TASK NO	WORK UNIT ACCESSION NO.

11. TITLE (Include Security Classification)
(U) DETERMINATION OF THE STRUCTURAL BASIS OF ANTIBODY DIVERSITY USING NMR

12. PERSONAL AUTHOR(S)
Harden M. McConnell

13a. TYPE OF REPORT ANNUAL	13b. TIME COVERED FROM 7/88 TO 7/89	14. DATE OF REPORT (Year, Month, Day) 89/6/15	15. PAGE COUNT

16. SUPPLEMENTARY NOTATION

17	COSATI CODES		18 SUBJECT TERMS (Continue on reverse if necessary and identify by block number)
FIELD	GROUP	SUB-GROUP	
06	03		

19 ABSTRACT (Continue on reverse if necessary and identify by block number)
Abstract: In collaboration with Michael Levitt we have constructed semiempirical/semitheoretical structural models of the twelve anti-nitroxide spin label antibodies previously sequenced in this laboratory. These models are in striking qualitative accord with the NMR difference spectra in showing the presence of a large number of aromatic amino acids (especially tyrosines) in the combining site region, i.e., within about 20 Å of the unpaired electron. The high motional freedom of the tyrosine residues (i.e., 10-12 residues in AN01-AN03) inferred from the NMR indicates that these residues play no significant role in maintaining a rigid three-dimensional structure of these proteins. We have determined the germline sequences of AN02 and AN07 and find similar numbers of tyrosine residues in the combining site regions. It is likely that the tyrosine and other residuees in the combining site regions that are highly mobile, and distributed over a large surface (≈ 20 Å x 20Å) are mostly designed for protein antigen recognition (not small haptens) including idiotype-anti-idiotype regulation. (U)

20. DISTRIBUTION/AVAILABILITY OF ABSTRACT [X]UNCLASSIFIED/UNLIMITED ☐ SAME AS RPT ☐ DTIC USERS	21 ABSTRACT SECURITY CLASSIFICATION (U)
22a. NAME OF RESPONSIBLE INDIVIDUAL M. Marron	22b. TELEPHONE (Include Area Code) 202/696-4760	22c. OFFICE SYMBOL ONR

DD Form 1473, JUN 86 Previous editions are obsolete SECURITY CLASSIFICATION OF THIS PAGE

S/N 0102-LF-014-6603

(U)

89 6 19 115

Distribution List for Annual and Final Reports

1. Put a cover page (Form DD 1473) on your report and attach a copy of the distribution list. Mail one copy of the report to each person on the contractor subset list attached on which your name appears. The other subset list is for your information only. Please don't forget to attach this distribution list to your report - otherwise the folks below think they have mistakenly received the copy meant for the Molecular Biology Program and forward it to us.

2. Mail two copies to (include a DTIC Form 50 with these two copies too)
    Administrator
    Defense Technical Information Center
    Building 5, Cameron Station
    Alexandria, VA 22314

3. Mail one copy to each of the following:

(a) Dr. Michael Marron
     ONR Code 1141
     Molecular Biology Program
     800 N. Quincy Street
     Arlington, VA 22217-5000

(b) Administrative Contracting Officer
     ONR Resident Representative
     (address varies - see copy of your grant)

(c) Director,
     Applied Research Directorate
     ONR Code 12
     800 N. Quincy Street
     Arlington, VA 22217-5000

(d) Director
     Office of Naval Technology
     Code 22
     800 N. Quincy Street
     Arlington, VA 22217-5000

(e) Director
     Chemical and Biological Sci Div
     Army Research Office
     P. 0. Box 12211
     Research Triangle Park, NC 27709

(f) Life Sciences Directorate
     Air Force Office of Scientific Research
     Bolling Air Force Base
     Washington, DC 20332

(g) Director
     Naval Research Laboratory
     Technical Information Div, Code 2627
     Washington, DC 20375

AMZEL, L. Mario
Department of Biophysics
Johns Hopkins School of Medicine
725 North Wolfe Street
Baltimore, MD 21205

ANDERSEN, Niels H.
Department of Chemistry
University of Washington
Seattle, WA 98195

ARNOLD, Frances H.
Dept of Chemical Engineering
California Institute of Technology
Pasadena, CA 91125

AUGUST, J. Thomas
Department of Pharmacology
Johns Hopkins Medical School
725 North Wolfe Street
Baltimore, MD 21205

BEVERIDGE, David L
Department of Chemistry
Wesleyan University
Hall-Altwater Laboratories
Middletown, CT 06457

BRAMSON, H. Neal
Department of Biochemistry
Univ of Rochester Medical Center
601 Elmwood Avenue
Rochester, NY 14642

BRUICE, Thomas C.
Department of Chemistry
University of California-Santa
Barbara
Santa Barbara, CA 93106

CASE, Steven T.
Department of Biochemistry
Univ of Mississippi Medical Center
2500 North State Street
Jackson, MS 39216-4505

CHANG, Eddie L.
Bio/Molecular Engineering
Naval Research Laboratory
Code 6190
Washington, D.C. 20375-5000

CHRISTIANSON, David W.
Department of Chemistry
University of Pennsylvania
231 South 34th Street
Philadelphia, PA 19104-6323

CORDINGLEY, John S.
Department of Molecular Biology
University of Wyoming
Box 3944 University Station
Laramie, WY 82071

DeGRADO, William F.
E. I. du Pont de Nemours & Co
Central R & D, Experimental Station
P. O. Box 80328
Wilmington, DE 19880-0328

EVANS, David R.
Department of Biochemistry
Wayne State Univ School of Medicine
540 E. Canfield Street
Detroit, Michigan 48201

FEIGON, Juli F.
Department of Chem & Biochemistry
UCLA
405 Hilgard Avenue
Los Angeles, CA 900024-1569

FICHT, Allison R.
Dept of Med Biochem & Genetics
Texas A&M University
College Station, TX 77843

FRAUENFELDER, Hans
Department of Physics
University of Illinois
Urbana, IL 61801

GABER, Bruce
Naval Research Laboratory
Bio/Molecular Engineering Branch
Code 6190
Washington, DC 20375

GETZOFF, Elizabeth D.
Scripps Clinic & Research Foundation
Department of Molecular Biology
10666 North Torrey Pines Road
La Jolla, CA 92037

GOODMAN, Eugene M.
Biomedical Research Institute
University of Wisconsin
P. O. Box 2000
Kenosha, WI 53141

HO, Pui Shing
Department of Biochemistry and
Biophysics
Oregon State University
Corvallis, OR 97331

HOGAN, Michael E.
Baylor Center for Biotechnology
4000 Research Forest Drive
The Woodlands, TX 77381

HONIG, Barry
Columbia University
Dept of Biochem and Molec Biophys
630 West 168th St.
New York, NY 10032

HOPKINS, Paul B.
Department of Chemistry
University of Washington
Seattle, WA 98195

KAHNE, Daniel
Department of Chemistry
Princeton University
Princeton, NJ 08544

KEMP, Robert G.
Chicago Medical School
Dept of Biological Chemistry
3333 Green Bay Rd.
North Chicago, IL 60064

KHORANA, Gobind H.
Department of Biology
MIT
77 Massachusetts Ave.
Cambridge, MA 02139

KIM, Sangtae
Chemical Engineering
University of Wisconsin
1415 Johnson Drive
Madison, WI 53706

LANSBURY, Peter T.
Department of Chemistry
MIT
Cambridge, MA 02139

LAURSEN, Richard A.
Chemistry Department
Boston University
590 Commonwealth Avenue
Boston, MA 02215

LENZ, Robert W.
Chemical Engineering Department
University of Massachusetts
Amherst, MA 01003

LEWIS, Randolf V.
Molecular Biology Department
University of Wyoming
University Station Box 3944
Laramie, WY 82071

LINDSAY, Stuart M.
Department of Physics
Arizona State University
Temp, AZ 85278

LOEB, George I.
David W. Taylor Research Center
Code 2841
Annapolis, MD 21402-5067

MASILAMANI, Divakar
Biotechnology Department
Allied-Signal Inc.
P. O. Box 1021R
Morristown, NJ 07960

McCONNELL, Harden M.
Stanford University
Department of Chemistry
Stanford, CA 94305

McELROY, Willam D.
Department of Chemistry
University of California - San Diego
La Jolla, CA 92093-0601

MERTES, Kristin Bowman
University of Kansas
Dept of Chemistry
Lawrence, Kansas 66045

NAGUMO, Mark
Bio/Molecular Engineering Branch
Naval Research Laboratory
Code 6190
Washington, DC 20375-5000

OLIVERA, Baldomero M.
Department of Biology
University of Utah
Salt Lake City, UT 84112

PABO, Carl O.
Department of Biophysics
Johns Hopkins University
School of Medicine
Baltimore, MD 21205

PRENDERGAST, Franklyn G.
Dept of Biochemistry & Molec Biol
Mayo Foundation
200 First St. SW
Rochester, MN 55905

PUGH, Jr., Edward N.
Deaprtment of Psychology
University of Pennsylvania
3815 Walnut Street
Philadelphia, PA 19104-6196

RACKOVSKY, Shalom R.
Department of Biophysics
University of Rochester
School of Medicine and Dentistry
Rochester, NY 14642

RAJAN, K. S.
Illinois Institute of Technology
Research Institute
10 W. 35th St.
Chicago, IL 60616

REINISCH, Lou
Laser Biophysics Center
Uniformed Services University
4301 Jones Bridge Road
Bethesda, MD 20814

RICH, Alexander
MIT Department of Biology
Cambridge, MA 02139

RICHARDS, J. H.
California Institute of Technology
Division of Chemistry and Chemical
Engineering
Pasadena, CA 91125

ROTHSCHILD, Kenneth J.
Department of Physics
Boston University
590 Commonwealth Avenue
Boston, MA 02215

SCHULTZ, Peter G.
Department of Chemistry
University of California-Berkeley
Bekeley, CA 94720

SEEMAN, Nadrian
Department of Chemistry
New York University
New York, NY 10003

SELSTED, Michael E.
UCLA
Dept of Medicine
37-055 CHS
Los Angeles, CA 90024

SIGMAN, David S.
UCLA School of Medicine
Dept of Biological Chemistry
Los Angeles, CA 90024

SIKES, Steven C.
Department of Biological Sciences
University of South Alabama
Mobile, AL 36688

SINSKEY, Anthony J.
Laboratory of Applied Microbiology
MIT Department of Biology
Cambridge, MA 02139

STEWART, James M.
Department of Chemistry
University of Maryland
College Park, MD 20742

STEWART, John M.
Department of Biochemistry
University of Colorado
Health Science Center
Denver, CO 80262

TURNER, Douglas H.
Department of Chemistry
University of Rochester
Rochester, NY 14627

URRY, Dan W.
Laboratory of Molecular Biophysics
University of Alabama
P. O. Box 311
Birmingham, AL 35294

WAITE, J. Herbert
College of Marine Studies
University of Deleware
Lewes, DE 19958

WARD, Keith B.
Naval Research Laboratory
Code 6030
Washington, DC 20375

WARSHEL, Arieh
Department of Chemistry
University of Southern California
University Park
Los Angeles, CA 90089-0482

WATT, Gerald D.
Dept of Chemistry & Biochemistry
University of Colorado
Campus Box 215
Boulder, CO 80309-0215

Line-Shape Analysis of NMR Difference Spectra of an Anti-Spin-Label Antibody[†]

Tom Frey,[‡] Jacob Anglister,[§] and Harden M. McConnell*[,‡]

Stauffer Laboratory for Physical Chemistry, Stanford University, Stanford, California 94305, and Polymer Department, The Weizmann Institute of Science, Rehovot 76100, Israel

Received October 14, 1987; Revised Manuscript Received March 14, 1988

ABSTRACT: Specifically deuteriated Fab fragments of the anti-spin-label antibody AN02 were prepared. NMR difference spectra were obtained, in which the spectrum of Fab with some fraction of the binding sites occupied with spin-label hapten was subtracted from the spectrum of Fab with no spin-label. The peak heights were analyzed as a function of the fractional occupation of the binding site, using a computer program that calculates a best fit to the observed spectra. This method treats all of the peaks in the spectra simultaneously. Analyzing all peaks at once allows for the interdependencies in the spectra arising from overlap of positive and negative signals from different peaks. The fitting program calculates line widths for the peaks arising from protons in the binding site region. Almost all of the line widths calculated for the spectrum of the Fab complex with diamagnetic hapten dinitrophenyldiglycine were found to be narrower than the line widths of the corresponding resonances in the spectrum of Fab with an empty binding site. The distances of the binding site region protons from the unpaired electron of the hapten were also obtained from this calculation. Two tyrosine protons were found to be close (<7 Å) to this electron. These line-width and distance results are discussed with respect to the structure and dynamics of the antibody binding site.

In an effort to improve the understanding of antibody binding site structure, we have pursued an NMR study of the anti-spin-label antibody AN02. In previous work, we used biosynthetic deuteriation and protein chemistry with NMR to obtain information about the amino acid makeup of the binding site region (Anglister et al., 1984a; Frey et al., 1984) and to assign resonances to the heavy and light chains (Anglister et al., 1985). Nuclear magnetization transfer was used to identify the resonances of protons in close proximity to the hapten (Anglister et al., 1987). The effect of the paramagnetic hapten on the protein NMR spectrum was used to measure the distance of certain antibody protons from the unpaired electron of the hapten (Anglister et al., 1984b).

The effect of the hapten on the AN02 resonance spectrum was described, and a technique for extracting distance information was discussed. This technique involves titrating the binding site of the Fab with paramagnetic hapten and sub-

tracting the NMR spectrum taken at each titration point from the spectrum of the Fab with no hapten bound. The change in peak height of each resonance was analyzed as a function of fractional occupation of the binding site. Several tyrosine resonances displayed the theoretically expected behavior.

The technique presented in our earlier paper analyzed one signal at a time, required that the line width of the proton resonance be known, and assumed that the resonance signals were homogeneous and Lorentzian. Of course, this is not satisfactory for spectra with multiple, overlapping resonances. Further difficulties arise with line-width determination when resonances are very broad or very narrow, due to low signal to noise and digitization, respectively. In the present work, we find that simulation and computer fitting of the observed spectra can be used successfully to extract the desired line-width and distance information.

MATERIALS AND METHODS

The preparation and purification of the AN02 antibody have been described. Fab fragments were prepared and purified as previously described. The affinity of AN02 for spin-label

has been reported to be 4×10^6 M^{-1} (Anglister et al., 1984a).

The Fab fragments used for the spectra in this paper were biosynthetically deuteriated in the tryptophan and phenylalanine residues, and in the 2- and 6-positions of the tyrosine rings. The only proton resonances seen in the spectral region of 6.0–9.0 ppm are therefore from the 3- and 5-protons of tyrosine and possibly from histidine. We have shown that histidine makes at most only a minor contribution to any of these difference spectra (Anglister et al., 1984b).

Three types of difference spectra were obtained. In the first type, the spectrum of Fab with spin-label bound was subtracted from the spectrum of Fab with an empty binding site. In the second type, the spectrum of Fab with spin-label bound was subtracted from Fab with dinitrophenyldiglycine (DNP) bound. In the third, the spectrum of Fab with spin-label bound was subtracted from that of Fab with chemically reduced spin-label bound. (In the reduced spin-label, the NO of the nitroxide group is replaced by the hydroxylamine group, NOH.) The chemical shifts of Fab proton resonances seen in this third type of spectrum were assumed to correspond to the chemical shifts in the Fab spin-label complex.

Two types of difference spectra titrations were recorded. In the "without minus with" titration, one subtracts the NMR spectrum of an Fab fragment in a given solution with spin-label from the spectrum of Fab in the absence of spin-label. Different difference spectra are recorded for different spin-label concentrations, corresponding to different fractional occupations of the combining site. In the "with DNP minus with spin label" titrations, one subtracts the NMR spectrum of an Fab fragment in a solution containing both spin-label *and* DNP-diglycine from the spectrum of a solution of Fab with (excess) DNP-diglycine from the spectrum of a solution of Fab with (excess) DNP-diglycine alone. The relative concentrations of spin-label and DNP-diglycine, together with their known binding constants, determine the fractional occupation of the binding site by each hapten. This relative fractional occupation is varied during the "with DNP minus with spin label" titration. Note that this second titration is distinct from that used earlier (Frey et al., 1984).

NMR spectra were simulated on an IBM-PC. Broadening due to the spin-label was described by the equations for paramagnetic broadening (Sternlicht et al., 1965a,b; Jardetzky & Roberts, 1981), giving an r^{-6} dependence for the effect (Solomon, 1955). Spectra for partially occupied situations were assumed to conform to the Bloch equations for one-proton, two-site exchange with an appropriate exchange rate (Gutowsky et al., 1953; McConnell, 1958). Rates found for these experiments are in a time regime intermediate between fast and slow exchange. Initial estimates for spectral parameters were improved by the Marquardt algorithm using a modification of the CURFIT routine of Bevington (1969). The programs were written in C, with time critical portions recoded in 8088 and 8087 assembly language, based on the assembly language output of the C compiler (Computer Innovations) [for further details, see Frey (1986)]. The spectra were digitized at 1-Hz intervals.

RESULTS

The best fit to the data uses an off rate of 430 s^{-1}. This gives a total squared deviation from the data of about 0.25% of the total squared amplitude. This fit is an order of magnitude better than when all distances are set equal to 10 Å and when the best-fit line widths are used. The value of 0.25% is probably set by the noise in the spectra. A further source of error may be the very low amplitude features that appear in the high-occupancy difference spectra and that are ignored by the fit.

The fitting algorithm used finds the parameters giving a minimum in the sum of the squares of the deviations of the calculated amplitudes from the observed data. The only free parameters in the model are the line width of the signal in the Fab with an unoccupied binding site, the line width of the same resonance in the with DNP complex, and the distance of the proton from the unpaired spin in the with spin-label complex. Thus, there are 3 parameters per proton to be fit in each data set (30 for the data set discussed in this paper). There is one observed amplitude per peak per titration point in the data set (108 points). Note that peak B is a composite of 2 signals (Anglister et al., 1985) and there are therefore 9 peaks and 10 protons. The fit is still overdetermined even for this many parameters, but the derived values for the two signals from peak B are given with less confidence. Further complicating the interpretation of peak B is the possibility of a third signal forming a shoulder on the high chemical shift side in difference spectra with high spin-label occupancy.

Some assumptions are implicit in the analysis of these NMR spectra. The scaling of the spectra assumes that at least one line width in one spectrum can be measured acurately. For the present calculations, the lines labeled H and G in the without minus with 100% spin-label spectrum were used for scaling all of the without minus with spin-label spectra. These special peaks were selected on the basis of the following criteria. (i) The location of the base line is clear. In these difference spectra, the summing of negative signals in regions with many resonances can affect the shape of the base line even when any one of these negative signals is too broad to make a noticeable effect. (ii) There is no overlap with other resonances. (iii) The protons are sufficiently near the unpaired electron that the contribution of the negative signal in the difference spectrum is completely obliterated at 100% occupancy. (Note that when proton signals of different width are subtracted the width at half-height of the resulting feature is not the line width of either proton signal.) (iv) The lines are narrow enough to provide good signal to noise but broad enough to provide enough data points to minimize error from the discontinuous nature of the digital spectrum. The measured line widths should also yield relative peak amplitudes that are consistent with those observed in the spectra. Using similar criteria, we used line H to scale the with DNP minus with with spin-label titration.

A second set of assumptions concerns the spectral position of resonances in the Fab spin-label complex. The chemical shifts of several tyrosine resonance change with the occupation of the binding site. Since these resonances are extremely broad in the spectrum of the Fab spin-label complex, it is not possible to determine the chemical shift directly. These shifts are therefore assumed to be the same as those observed in the complex with reduced spin-label. The chemical shifts of resonances in the reduced spin-label complex are very similar to those in the DNP complex, and so this likely to be a good approximation (Anglister et al., 1985).

Another question arises when treating the with DNP minus with spin-label spectra. The system was analyzed as a two-state system involving only the DNP complex and the spin-label complex. The concentrations of DNP and spin-label were kept high enough to saturate all the binding sites, and the concentration of Fab was high enough to make the concentration of free Fab negligible. The Appendix shows that under these conditions a three-state NMR line-shape problem is reduced to the two-state treatment used.
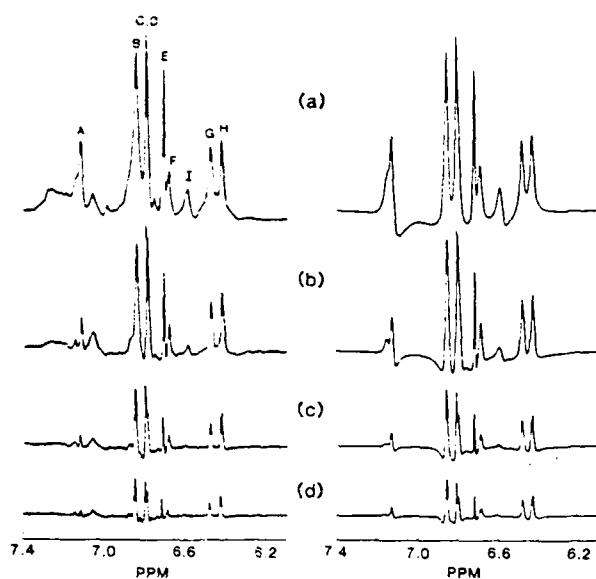
FIGURE 1: Difference spectra of without spin-label minus with spin-label. The spectra at the right are simulations, and the spectra at the left are the observed spectra. The binding site occupancies with spin-label are (a) 100%, (b) 20.03%, (c) 4.96%, and (d) 2.57%.
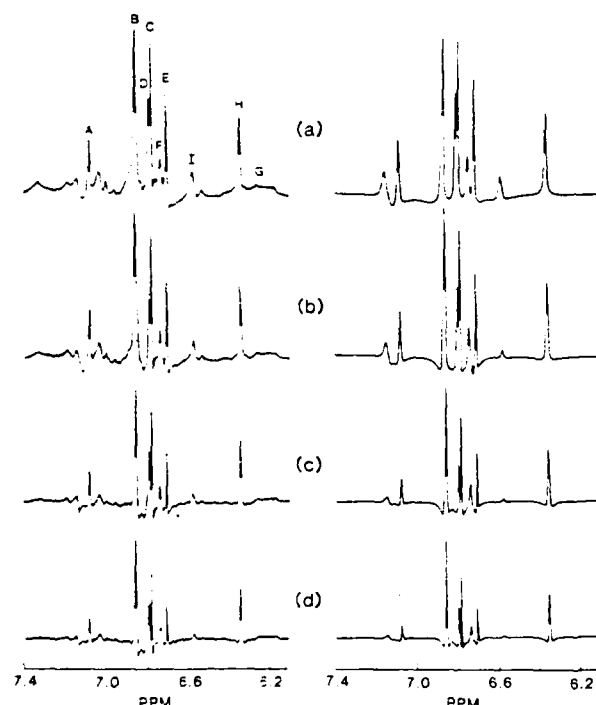

FIGURE 2: Difference spectra of with DNP minus with spin-label. The spectra at the right are simulations, and the spectra at the left are the observed spectra. The binding site occupancies with spin-label are (a) 100%, (b) 25.2%, (c) 7.52%, and (d) 3.9%.

Figure 1 shows the simulated and observed spectra for several of the difference spectra in the without minus with spin-label titration. All spectra are to the same scale. Figure 2 shows results for the with DNP minus with spin-label titration. The spectra in Figures 1 and 2 are to different scales. Only four of the six recorded spectra in each data set are shown. The spectra for the third and fifth highest occupancy are omitted in each case.

The changes in chemical shift that occur on binding can be observed by comparing Figure 1a and Figure 2a. These changes make the amplitudes of pairs of lines interdependent in several cases. The lines labeled C and D are very close to each other, and the negative signals from each of these protons

Table I: Spectral Parameters for without minus with Spin-Label Titration

proton	chemical shift[a] (ppm)	line width[a] (Hz)
A	7.126	9.4
B1	6.864	6.9
B2	6.857	7.7
C	6.810	5.1
D	6.799	8.4
E	6.722	4.8
F	6.693	12.1
G	6.487	10.8
H	6.435	10.2
I	6.595	17.0

[a] The chemical shifts and line widths individually do not have any significance beyond ±0.01 ppm and ±1 Hz. The shapes of overlapping signals are more sensitive to the relative values of line positions and widths than these limits, as indicated by the number of significant figures used in the table.

Table II: Spectral Parameters for with DNP minus with Spin-Label Titration

proton	chemical shift[a] (ppm)	line width[a] (Hz)
A	7.082	5.8
B1	6.865	6.0
B2	6.865	2.9
C	6.784	2.8
D	6.795	4.2
E	6.706	3.3
F	6.738	8.25
G	6.135	br[b]
H	6.349	5.15
I	6.575	11.0

[a] The chemical shifts and line widths individually do not have any significance beyond ±0.01 ppm and ±1 Hz. The shapes of overlapping signals are more sensitive to the relative values of line positions and widths than these limits, as indicated by the number of significant figures used in the table. [b] Broad.

affect the other's amplitude in one or both of the titrations. The negative feature from line F moves through the position of the positive signal from line E in the without minus with spin-label titration, thus affecting its amplitude. The fitting algorithm allows for these interdependencies. It is more difficult to model the small signal at slightly higher chemical shift than line A and its effect on the observed amplitude of line A. This is probably not a tyrosine signal (or even necessarily from a single source). Both histidine and unexchanged peptide amide protons would show signals in this spectral region. Since the number of protons giving rise to this signal cannot be determined, it cannot be scaled properly with respect to the tyrosine signals in the calculation.

Table I lists spectral parameters derived from the without spin-label minus with spin-label spectra. The chemical shifts of the protein tyrosine resonances and the line widths derived from the best fit to the titration data are shown in the table. Table II shows results for the with DNP minus with spin-label difference spectra. Identical labels for the protons in the two tables indicated that the protons are from the same amino acid. The method used to interrelate signals in the two spectra has been discussed previous (Anglister et al., 1984). Note that the line widths of a given proton are not the same in the two types of spectra and are almost always narrower in the DNP complex. Examination of the spectra in Figures 1 and 2 shows that the line shapes calculated are in most cases in good agreement with the observed spectra, so that this difference in calculated line width is not likely to be an artifact of the different scaling of the two titrations.

This narrowing of line width in the with DNP spectrum is interesting. If some paramagnetic impurity is less able to penetrate the protein when hapten is bound, a narrowing effect

Table III: Results with Relevance to Model Building

proton	change in chemical shift (without spin-label to with DNP in ppm)	distance[a] (Å)	chain
A	0.044	12.9	H
B1	-0.001	12.3	H
B2	-0.001	<7	H
C	0.026	11.5	L
D	0.004	9.0	L
E	0.016	13.7	H
F	-0.045	10.85	L
G	0.352	ND[b]	L
H	0.086	<7	H
I	0.020	16.0	L

[a] The calculated distances are derived from averages of the inverse sixth power of the electron spin–proton spin distance and may represent averages over different molecular conformations. [b] Not determined.

might be observed. We have accumulated spectra in the presence and absence of dissolved oxygen and see no difference in line width, ruling out the most likely candidate for the broadening agent. A second possibility is that there is more mobility for tyrosine residues not in contact with the hapten when hapten is bound. We have previously stated that the large number of resonances showing some change in chemical shift might indicate a significant change in average conformation. On the other hand, there is clearly an immobilizing effect on the tyrosine giving rise to resonance G, along with the very large change in chemical shift seen for this resonance.

Table III shows the change in chemical shift undergone by each Fab tyrosine resonance upon DNP binding. This table also shows the calculated distance of each of these protons from the paramagnetic center of the hapten. Distances of less than 7 Å cannot be resolved because of the magnitude of the off rate of the hapten (Anglister et al., 1984), and are all labeled as <7. The change in chemical shift and the distance from the spin are the two parameters with strongest implications for structural models of the antibody. An L or H is included in the last column to indicate a light- or heavy-chain origin for the resonance (Anglister et al., 1985). The distances given here are in agreement with those reported previously (Anglister et al., 1984), except for line D. The overlap in line D with line C is likely to be a source of error in the previous calculations.

The value for the distance of line G from the paramagnetic center could not be determined. This is due to the large change in chemical shift undergone by this signal during the without minus with spin-label titration. The negative signal from the partially occupied spectrum moves out from under the positive signal at very low occupancy and is exchange broadened independent of any paramagnetic effect. A distance value for protons giving rise to signal G cannot be obtained from the with DNP minus with spin-label titration due to the extremely poor signal to noise for this line caused by its large line width.

DISCUSSION

It can be seen from the simulated spectra (Figures 1 and 2) that the computer analysis used in this work gives a good approximation to the observed spectra. The simulation of the spectra allows the analysis of overlapping signals. The rate of appearance of a resonance in a titration is dependent on the line width, but line-width measurements are not very accurate when determined directly from the spectra. Spectral simulation forces the line widths to be mutually consistent. The derived line widths also provide a quantitative confirmation of the qualitative observation that resonances in the

DNP complex are narrower than in the free Fab, as discussed under Results.

The spectra discussed here yield results with structural implications. We have previously discussed a computer model of the antibody and used it to assign likely tryptophan residues to specific resonances (Anglister et al., 1987). The assignment of tyrosine resonances is not so straightforward. There are two heavy-chain tyrosines (33 and 50) which are candidates for signals B and H, but the large number of tyrosine residues makes this assignment very provisional. Further complicating the situation is the lack of an obvious candidate for resonance G. This is the tyrosine resonance that undergoes a large change in chemical shift upon hapten binding. One reason for the lack of a candidate is that the model was computed for an empty binding site, and the change in chemical shift could be due to conformational change in the Fab. There are at least four light-chain tyrosine residues that could be candidates under these assumptions, including the three tyrosines in the second hypervariable loop of the light chain.

The type of analysis described here is being applied to titrations done with several different deuterations. It is hoped that a collection of these measurements will lead to an understanding of the solution structure of this antibody and, in conjunction with the crystallographic and mutagenesis studies under way, will lead to an improved understanding of antibody–hapten binding in terms of both structure and kinetics.

APPENDIX

Magnetization Transfer Due to Chemical Exchange. The chemical components of the system are Fab, spin-label (SL), DNP-diglycine (DNP), and the complexes of Fab with spin-label (FabSL) and of Fab with DNP (FabDNP). Two reversible reactions are assumed:

$$FabSL \rightleftharpoons Fab + SL \qquad (1)$$
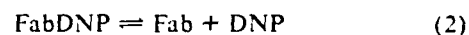
$$FabDNP \rightleftharpoons Fab + DNP \qquad (2)$$

Thus, we assume that FabSL can only be converted to FabDNP through the intermediate free Fab.

Let M_S be the macroscopic magnetization association with a specific proton in the Fab fragment when spin-label is bound and M_D be the magnetization of the same proton when DNP is bound. Let M_0 be the magnetization of this proton when the binding site is empty. The changes of the macroscopic magnetization due to chemical exchange can then be written as follows:

$$\dot{M}_S = -k_{S0}M_S + k_{0S}M_0 \qquad (3)$$

$$\dot{M}_D = -k_{D0}M_D + k_{0D}M_0 \qquad (4)$$

$$\dot{M}_0 = -k_{0S}M_0 - k_{0D}M_0 + k_{S0}M_S + k_{D0}M_D \qquad (5)$$

where k_{S0} is the first-order rate constant for dissociation of the Fab–spin-label complex and k_{0S} is the pseudo-first-order rate constant for reassociation.

Assume experimental conditions where there is always an excess of spin-label and/or DNP such that the binding sites of the Fab fragments are almost always occupied. Under these circumstances, the concentration of free Fab is very small, and we may set $M_0 = 0$. We then obtain the following expression for M_0:

$$M_0 = \frac{k_{S0}M_S + k_{D0}M_D}{k_{0S} + k_{0D}} \qquad (6)$$

Substitution of this expression for M_0 in eq 3 and 4 allows these equations to be rewritten as
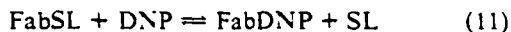
$$M_S = -k_{SD}M_S + k_{DS}M_D \tag{7}$$

$$M_D = -k_{DS}M_D + k_{SD}M_S \tag{8}$$

where

$$k_{SD} = \frac{k_{S0}k_{0D}}{k_{0S} + k_{0D}} \tag{9}$$

$$k_{DS} = \frac{k_{D0}k_{0S}}{k_{0S} + k_{0D}} \tag{10}$$

Thus, the equations describing the change of magnetization due to chemical exchange have the form of a two-site exchange reaction, as though the reaction

$$FabSL + DNP \rightleftharpoons FabDNP + SL \tag{11}$$

took place with rate constants k_{SD} and k_{DS}.

In the form of the Bloch equations described in Wien et al. (1972), the parameter τ is used, and for the present problem

$$\tau = 1/k_{SD} + 1/k_{DS} \tag{12}$$

In order to put this equation into useful form, we can express the time τ in terms of the true first-order off rate constants k_{S0} and k_{D0} and the fractional occupation of the binding site by spin-label and DNP, namely, f_S and f_D. To do this, first note that

$$k_{0S} = k'_{0S}[SL] \tag{13}$$

$$k_{0D} = k'_{0D}[DNP] \tag{14}$$

where k'_{0S} and k'_{0D} are the true second-order rate constants for the reverse reactions in eq 1 and 2. The equilibrium constant for reaction 1 is

$$K_S = \frac{[Fab][SL]}{[FabSL]} = \frac{k_{S0}}{k'_{0S}} \tag{15}$$

and for reaction 2

$$K_D = \frac{[Fab][DNP]}{[FabDNP]} = \frac{k_{D0}}{k'_{0D}} \tag{16}$$

By combining eq 15 and 16 with eq 12, we obtain the following expression:

$$\tau = \frac{1}{f_D k_{D0}} + \frac{1}{k_{S0}f_S} \tag{17}$$

or

$$\tau = \tau_{D0}/f_D + \tau_{S0}/f_S \tag{18}$$

where τ_{D0} and τ_{S0} are the lifetimes for the two haptens in the combining site. (Note that for the two-site exchange case, where there is no DNP-diglycine, $\tau = 1/k_{S0}f_S$. The effect of the DNP-diglycine is effectively to slow down the rate of entry of the spin-label into the binding site.)

Registry No. DNP-glycine, 1084-76-0.

REFERENCES

Anglister, J., Frey, T., & McConnell, H. M. (1984a) *Biochemistry 23*, 1138–1142.

Anglister, J., Frey, T., & McConnell, H. M. (1984b) *Biochemistry 23*, 5372–5375.

Anglister, J., Frey, T., & McConnell, H. M. (1985) *Nature (London) 315*, 65–67.

Anglister, J., Bond, M. W., Frey, T., Leahy, D., Levitt, M., McConnell, H. M., Rule, G. S., Tomasello, J., & Whitaker, M. (1987) *Biochemistry 26*, 6058–6064.

Bevington, P. R. (1969) *Data Reduction and Error Analysis for the Physical Sciences*, McGraw-Hill, New York.

Frey, T. (1986) Ph.D. Thesis, Stanford University.

Frey, T., Anglister, J., & McConnell, H. M. (1984) *Biochemistry 23*, 6470–6473.

Gutowsky, H. S., McCall, D. W., & Slichter, C. P. (1953) *J. Chem. Phys. 21*, 279.

Jardetzky, O., & Roberts, G. C. K. (1981) *NMR in Molecular Biology*, Academic, New York.

McConnell, H. M. (1958) *J. Chem. Phys. 28*, 430–431.

Solomon, I. (1955) *Phys. Rev. 99*, 559–565.

Sternlicht, H., Shulman, R. G., & Anderson, E. W. (1965a) *J. Chem. Phys. 43*, 3133–3143.

Sternlicht, H., Shulman, R. G., & Anderson, E. W. (1965b) *J. Chem. Phys. 43*, 3123–3132.

Wien, R. W., Morrisett, J. D., & McConnell, H. M. (1972) *Biochemistry 11*, 3707–3716.

Sequences of 12 monoclonal anti-dinitrophenyl spin-label antibodies for NMR studies

DANIEL J. LEAHY, GORDON S. RULE, MEI M. WHITTAKER, AND HARDEN M. MCCONNELL

Stauffer Laboratory for Physical Chemistry, Stanford University, Stanford, CA 94305

ABSTRACT   Eleven monoclonal antibodies specific for a spin-labeled dinitrophenyl hapten (DNP-SL) have been produced for use in NMR studies. They have been named AN01 and AN03–AN12. The stability constants for the association of these antibodies with DNP-SL and related haptens were measured by fluorescence quenching and ranged from 5.0×10^4 M^{-1} to $>1.0 \times 10^8$ M^{-1}. cDNA clones coding for the heavy and light chains of each antibody and of an additional anti-DNP-SL monoclonal antibody, AN02, have been isolated. The nucleic acid sequence of the 5' end of each clone has been determined, and the amino acid sequence of the variable regions of each antibody has been deduced from the cDNA sequence. The sequences are relatively heterogeneous, but both the heavy and the light chains of AN01 and AN03 are derived from the same variable-region gene families as those of the AN02 antibody. AN07 has a heavy chain that is related to that of AN02, and AN09 has a related light chain. AN05 and AN06 are unrelated to AN02 but share virtually identical heavy and light chains. Preliminary NMR difference spectra comparing related antibodies show that sequence-specific assignment of resonances is possible. Such spectra also provide a measure of structural relatedness.

Many different magnetic resonance techniques can be used to gain structural information about antibodies in solution (1). The combining sites of antibodies specific for spin-labeled molecules are particularly accessible to study by nuclear magnetic resonance (NMR). The spin-label broadens the NMR signals of nearby (<17 Å) protons in a strongly distance-dependent manner. A simple NMR difference spectrum, antibody alone minus antibody with bound spin-label, is dominated by resonances from protons that are near the electron spin. Anglister et al. (2) used this effect to gain information about the amino acid composition of the binding site of AN02, a monoclonal antibody raised against a spin-labeled dinitrophenyl hapten (DNP-SL). Growth of the AN02-producing cell line in medium containing selected deuterated amino acids results in virtually complete incorporation of these deuterated amino acids into the antibody. This selective deuteration permits the assignment of resonances to specific amino acid types. Considerable simplification of spectra is afforded through the use of partially deuterated amino acids to remove splitting of the resonances. Measurement of the broadening effect of the spin-label on specific resonance signals at various binding-site occupancies allows the calculation of the distance between these protons and the electron spin. A complication in this type of distance measurement arises if the spin-label adopts more than one conformation relative to the protein (3). An electron paramagnetic resonance spectrum of AN02 with the spin-label hapten shows the spin-label to be tumbling at the same rate as would be expected for AN02 (2). The distances from the spin-label of seven AN02 tyrosines were measured by

varying the amount of spin-label in the binding site (4). Such distance measurements were also made for resonances arising from alanine, isoleucine, leucine, threonine, and valine (G.S.R., D.J.L., and H.M.M., unpublished data). Recombination of heavy and light chains with different deuterations has allowed identification of the chain of origin of these tyrosine signals (5). Nuclear magnetization transfer measurements were used to identify resonance signals from two tryptophans in AN02 that must be <5 Å from the hapten (6).

The NMR lineshapes provide information about the binding-site dynamics. The linewidths of resonance signals originating from residues on the surface of AN02 indicate that these residues are moving much faster than the entire Fab molecule. The linewidths of peaks corresponding to the tyrosine residues for which distance measurements were made varied from 5 to 15 Hz. The sharpness of signals from binding-site protons greatly simplifies analysis of NMR spectra from a protein as large as an Fab fragment. The change in linewidth of a resonance in the AN02 NMR spectrum upon binding of a diamagnetic hapten was used to measure the off-rate for this hapten (4).

Given the available distance information about amino acids near the spin-label in AN02, sequence-specific assignment of resonance signals will enable construction of a working model of the combining site. We believe that such sequence-specific assignments can be obtained in part by using monoclonal antibodies differing from AN02 by a small number of amino acids. We have thus constructed a panel of 12 monoclonal antibodies that bind the DNP-SL hapten. We have also isolated and sequenced cDNA clones for both chains of each of these antibodies.* These clones enable creation of related antibodies through site-directed mutagenesis, genetic mixing and matching of heavy and light chains, and construction of hybrid variable (V) regions. Preliminary data given below demonstrate NMR difference spectra between closely related antibodies to be a viable technique to obtain sequence-specific assignments.

The Fab fragment of the AN02 antibody forms cocrystals with the DNP-SL hapten that diffract to high resolution (D.J.L., H.M.M., and R. O. Fox, unpublished data). The solution of the AN02 crystal structure will provide an opportunity to compare NMR and x-ray structural information for antibody–hapten complexes.

MATERIALS AND METHODS

Immunization of Mice. Six- to 8-week old female BALB/c mice were given intraperitoneal injections of the DNP-SL hapten coupled to 250 µg of bovine serum albumin (DNP-SL-BSA) in a 1:1 emulsion with complete Freund's adjuvant. The DNP-SL-BSA complex was prepared by the method

---

Abbreviations: DNP-SL, spin-labeled dinitrophenyl; C, constant; D, diversity; J, joining; V, variable.
*The sequences reported here are being deposited in the EMBL, GenBank data base (IntelliGenetics, Mountain View, CA, and Eur. Mol. Biol. Lab., Heidelberg) (accession nos. J03832 and J03833).

Chemistry: Leahy *et al.*

Proc. Natl. Acad. Sci. USA 85 (1988)   3663

Table 1. Characteristics of the monoclonal antibodies

Name	KH	KL	H	L	J_H	J_L	Stability constant, M^{-1}						
							DNP-SL	DNP-SG	DNP-G$_2$	DNP-SA	DNP-D$_2$	DNP-en$_2$	DNP-G
AN01	Ia	VI	γ1	κ	J_H2	$J_\kappa4$	5.1×10^4						
AN02	Ia	VI	γ1	κ	J_H3	$J_\kappa5$	7.5×10^6	1.8×10^7	3.1×10^6	2.0×10^7	2.7×10^5	6.0×10^6	4.5×10^6
AN03	Ia	VI	γ1	κ	J_H2	$J_\kappa5$	6.2×10^4	Low	Low				
AN04	IIa		γ1	κ	J_H3	$J_\kappa1$	6.8×10^6	4.4×10^7	2.2×10^6	2.9×10^6	Low		
AN05	IIc	II	γ1	κ	J_H2	$J_\kappa5$	9.5×10^6	9.2×10^6	Low	1.2×10^7			
AN06	IIc	II	γ1	κ	J_H2	$J_\kappa5$	1.2×10^7	2.7×10^7	Low	2.6×10^7			
AN07	Ia	I	γ1	λ	J_H3	$J_\lambda1$	2.5×10^7	$>5 \times 10^7$	4.9×10^5	9.7×10^5	Low		
AN08	IIa	V	γ1	κ	J_H4	$J_\kappa2$	7.3×10^7	3.0×10^7	1.7×10^6	2.4×10^6	Low		
AN09	IIa	VI	γ2a	κ	J_H3	$J_\kappa5$	1.6×10^7	$>1 \times 10^8$	4.0×10^7	$>1 \times 10^8$	2.7×10^6		
AN10	III	I	γ1	λ	J_H4	$J_\lambda1$	4.9×10^7						
AN11	IIa	V	γ1	κ	J_H1	$J_\kappa2$	5.0×10^5						
AN12	IIa	V	γ1	κ	J_H3	$J_\kappa2$	2.1×10^6						

Subgrouping [according to Kabat *et al.* (12)] for the heavy (KH) and light (KL) chain, isotype for the heavy (H) and light (L) chain, J-region usage for the heavy (J_H) and light (J_L) chain, and stability constant for various DNP haptens are shown for each antibody. The haptens were as follows: DNP-TEMPO-ethylenediamine (DNP-SL), DNP-TEMPO-glycine (DNP-SG), DNP-bis(glycine) (DNP-G$_2$), DNP-TEMPO-aspartic acid (DNP-SA), DNP-bis(aspartic acid) (DNP-D$_2$), DNP-bis(ethylenediamine) (DNP-en$_2$), DNP-glycine (DNP-G). TEMPO is 2,2,6,6-tetramethyl-1-oxypiperidin-4-yl. All haptens were synthesized by amine linkage of the substituents to the 2 and 4 positions of 2,4-difluoro-1,5-dinitrobenzene except DNP-glycine, which was purchased from Sigma.

extended to the *Eco*RI site at positions 3559–3564 of the *J–C* intron. This termination site is probably an artifact of our size selection and inadequate methylation during construction of the libraries. These transcripts are probably nonfunctional, as they contain several in-frame stop codons. The presence of this clone in a library expressing a γ2a heavy chain indicates that it is not solely due to missplicing of the expressed transcript. The aberrant γ sequence constituted ≈10% of γ clones screened from all libraries.

Sequencing of multiple clones revealed occasional differences between clones encoding the same polypeptide chain. Of ≈25,000 overlapping sequence measurements, 4 single-base-pair substitutions were detected. The errors appeared to be random and indicated a small but nonnegligible error rate (on the order of 1 error per 6000 base pairs) in our cloning procedures.

A 7-base-pair insertion was observed in one of the clones coding for the AN04 κ chain. The correct sequence at the insertion site, as determined from two independent clones, consisted of a contiguous repeat of the 7-base-pair sequence 5′ d(CAGCCTG) 3′. In the abnormal clone this sequence was repeated three times, suggesting a slippage or "hiccup" of the polymerase during chain elongation. Error due to the slipping of a polymerase between direct repeats has been postulated as a mechanism of somatic mutation in immunoglobulins (15).

A series of abnormalities was also observed in the leader sequence of AN02 heavy chain clones near the initiating

FIG. 1. Deduced amino acid sequences of the V regions of the heavy chains of the anti-DNP-SL monoclonal antibodies AN01–AN12. Numbering system is according to Kabat *et al.* (12). Standard one-letter amino acid symbols are used.

```
              -20      -10        1        10       20      27
               I        I         I        I        I       I ABCDEF
     ANO2      MDFQVQIFSFLLISASVILSRGQIVLTQSPAIMSASPGEKVTMTCSASS
     ANO1      ..............M.....M.................L..........
     ANO3      ...........M.....M...................L...........
     ANO9      ............I..VM...EN.........I...L......S.R....
     ANO5      MRCSLQFLGVLMFWISGVS.D..I..DELSNPVAS..S.SIS.RSTKSLL
     ANO6      MRCSLQFLGVLMFWISGVS.D..I..DELSNPVTS..S.SIS.RSTKSLL
     ANO4      MR.LAELLG.LLFCFLGV.CD.QMN...SSL...L.DTI.I..H..Q
     ANO8      MRF.VQVLG.LLLWISGAQCDVQI....SYLA.....TIIIN.R..K
     AN11      MVFTPQILG.MLFWISA...D.......TL.VT..DS.SLS.R..Q
     AN12      MHHTSMGIKMES..QV.VFVFLWLSGVD.D..M...HKF..T.V.DR.SI..K..Q
     ANO7      MAW.SLI.SLL.LSSGAIS.A.V..ES. LTT....T..L..RS.N
     AN10      MAW.SLI.SLL.LSSGAIS.A.V..ES. LTT....T..L..RS.T
```

```
               30       40       50       60     .. 70      80
               I        I        I        I        I        I
     ANO2      SVYYMYWYQQKPGSSPRLLIYDTSNLASGVPVRFSGSGSGTSYSLTISRMEAEDAA
     ANO1      ..S..F......R...KPW..L..........A..............S.......
     ANO3      ..S..F......R...KPW.FL.........A....R...........S.......
     ANO9      ..N..F......SDA..K.W..Y....P...A.........N........S.AG....
     ANO5      YK DGKT.LN.FL.R..Q..Q....LM.TR....SD.........DFT.E...VK...VG
     ANO6      YK DGKT.LN.FL.R..Q..Q....LM.TR....SD.........DFT.E...VK...VG
     ANO4      NINVWLS........NI.K....KA...HT...S...........FT....SLQP..I.
     ANO8      SISK.LA...E...KTNK...SG.T.Q..I.S..........DFT....SL.P..F.
     AN11      SVSNNLH.F...SHE......KYA.QSI..I.S.........DFT.S.NSV.T..FG
     AN12      DVSTAVA.......Q..K....SA.YRYT...D..T.......DFTF...SVQ...L.
     ANO7      GAVTTSN.AN.V.E..DHLFTG..GG.N.R.P...A.....LI.DKAA...TGAQT..E.
     AN10      GAVT.SNSVK.V.E..DHLFTG..GGSN.R.P...A.....LI.DKAA...AGAQT..E.
```

```
               90    95          100    106 109
               I      ABCDEF       I      A  I
     ANO2      TYYCQQWSSYPP      ITFGVGTKLEL KRA
     ANO1      ..........N..     ....S.....I ...
     ANO3      .......N.I..      ....A...... ...
     ANO9      ......FT.S.       S...A...... ...
     ANO5      V.....LVEF.       L...A...... ...
     ANO6      V.....LVEF.       L...A...... ...
     ANO4      ......GQ...       L.L.G.....I ...
     ANO8      M.....HNE..       Y...G.....I ...
     AN11      M.F...SN.W.       F...G.....I ...
     AN12      V...H.HY.S.       Y...G.....I ...
     ANO7      I.F.AL.Y.NH       LV..G....TVLGQP
     AN10      V.F.AL.Y.NH       LV..G.A..TVLGQP
```

Fig. 2. Deduced amino acid sequences of the V regions of the light chains of the anti-DNP-SL monoclonal antibodies AN01–AN12. Numbering system is according to Kabat *et al.* (12).

ATG. Of four independent cDNA clones sequenced, three different sequences were found in this region (Fig. 4), one of which was identical to the sequence of this region from a genomic clone of the AN02 heavy chain. Plasmids containing the non-germ-line versions of this gene appear to lyse the host bacteria before saturating growth conditions are reached.

DISCUSSION

In Fig. 5, spectra a and b show the aromatic regions in an NMR difference spectrum, unoccupied Fab minus Fab occupied with a low concentration of DNP-SL, for AN05 and AN06, respectively: The signals in these spectra originate from protons in close proximity to the spin-label (<10 Å). There is only one sequence difference between AN05 and AN06 variable regions that involves aromatic residues. AN05 has a tyrosine at position 94 of the heavy chain, whereas AN06 has a histidine at this position. Spectrum c is the double difference spectrum obtained by subtracting spectrum b from spectrum a. This spectrum clearly reveals four negative signals, which are likely to arise from the tyrosine-94 protons of AN05, and two positive signals, which are candidates to

arise from the histidine-94 protons of AN06. The upfield chemical shift of the positive features is unusual for histidine residues but not without precedent (16). Further experiments, such as selective deuteration, are necessary before a detailed interpretation of these spectra can be made.

The simplicity of the double difference spectrum, c, in Fig. 5 shows that the binding sites of AN05 and AN06 have nearly identical conformations. This result illustrates how simple NMR difference spectra can provide a useful measure of the structural relatedness between antibodies of highly similar sequence. This approach may also be of use for other families of closely related proteins for which a limited number of structures are known.

Both AN05 and AN06 have a yellow color after elution from a protein A-Sepharose column. This coloring could not be removed by extensive dialysis. Preliminary experiments show this color to be due to bound riboflavin, presumably from the culture medium. AN05 and AN06 also bind flavin mononucleotide and flavin adenine dinucleotide. This binding of DNP-SL and these flavins is competitive.

AN01 and AN03 are similar enough in sequence that NMR difference spectra, in combination with deuteration, should yield some sequence-specific assignments. AN01 and AN03
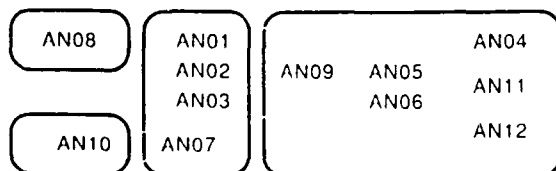
```
  AN08      AN01              AN04
            AN02   AN09  AN05
            AN03         AN06  AN11
  AN10      AN07              AN12
```

Fig. 3. AN01–AN12 grouped according to those that have closely related chains. Dark lines enclose antibodies whose heavy-chain nucleic acid sequences are >75% identical. Lighter lines enclose antibodies whose light-chain nucleic acid sequences are >85% identical. A different criterion was used for heavy chains because this distinction provided the clearest discrimination between sequences.

```
                 -17  -16  -15  -14  -13  -12
   1.  GCC TAA  AAG  ATG AGA GTG CTG ATT CTT
   2.  CAG CCT  CCA  GTG AGA GCG ATG ATT CTT
   3.  CAG CCT  CCA  GTG AGA GCG CTG ATT CTT
```

Fig. 4. Nucleic acid sequences of the leader regions of different cDNA clones encoding the AN02 heavy chain. The codons are numbered relative to the last residue of the leader peptide (−1). The sequences 3' to those shown were identical among all clones and coded for an otherwise normal heavy chain. Sequence 1 is identical to the sequence for this region found in a genomic clone of the AN02 heavy chain. Sequence 2 was found in two independent cDNA libraries constructed from different preparations of RNA. Sequence 3 did not contain an apparent initiating ATG codon. These differing leaders do not arise from an identifiable splicing event (14).
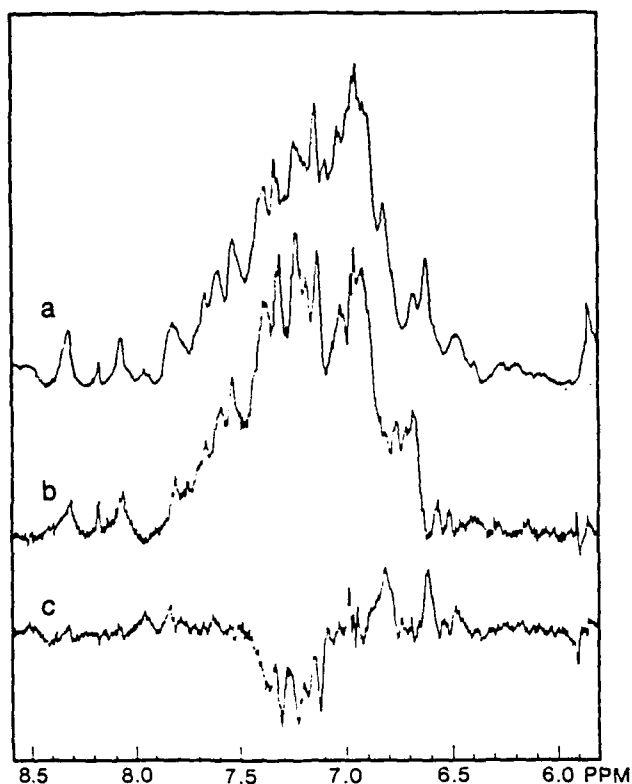
FIG. 5. Aromatic regions of the difference spectra, unoccupied Fab minus Fab with 4% (mol/mol) bound spin-label, for AN06 (spectrum a) and AN05 (spectrum b). Spectrum c is the double difference spectrum a minus b.

differ enough from AN02 that direct comparison of NMR spectra is unlikely to yield sequence-specific assignments for AN02. The number of amino acid differences in the *V* regions and the use of different leader sequences indicate that both chains of AN02 are derived from related but different germ-line genes as those of AN01 and AN03. AN02 has 100-fold higher affinity for DNP-SL than do AN01 and AN03. Site-directed mutagenesis should allow identification of residues important for high-affinity binding in these related antibodies. Cloning and sequencing of the germ-line genes that gave rise to the AN02 *V* regions should enable the construction of mutants for investigation of structural pathways selected during somatic mutation.

The remaining antibodies use unique combinations of heavy and light chains. The diversity found in these anti-DNP-SL antibodies provides a rich source for structural and functional studies. The creation of new antibodies with recombinant techniques further increases the diversity of this system. Mixing and matching heavy and light chains combinatorially increases the number of related antibodies within a subgroup and provides for chain-specific assignments. Restriction endonuclease sites can be used to create hybrid chains. For example, restriction sites in the third framework region of the heavy chain allow switching of the *D-J* combination in cases where similar *V*, but different *D* and *J*, regions are used.

NMR studies provide kinetic information in a time range particularly relevant to hapten binding (H.M.M., T. E. Frey, and J. Anglister, unpublished data). Construction of mutants that affect the on-rates or the off-rates of specific haptens should reveal structural features relating to chemical kinetics (17).

The NMR techniques used to study the combining sites of monoclonal anti-spin-label antibodies can clearly be extended to other proteins with modest affinities for spin-labeled ligands. Modification of ligands with spin-labels, in combination with amino acid deuteration and recombinant DNA techniques, promises to allow detailed analyses of protein binding sites by NMR.

1. Dwek, R. A., Wain-Hobson, S., Dower, S., Gettins, P., Sutton, B., Perkins, S. J. & Givol, D. (1977) *Nature (London)* 266, 31–37.
2. Anglister, J., Frey, T. & McConnell, H. M. (1984) *Biochemistry* 23, 1138–1142.
3. Leigh, J. S. & McLaughlin, A. C. (1979) in *NMR and Biochemistry*, eds. Opella, S. J. & Lu, P. (Dekker, New York), pp. 345–356.
4. Anglister, J., Frey, T. & McConnell, H. M. (1984) *Biochemistry* 23, 5372–5375.
5. Anglister, J., Frey, T. & McConnell, H. M. (1985) *Nature (London)* 315, 65–67.
6. Anglister, J., Bond, M. W., Frey, T., Leahy, D. J., Levitt, M., McConnell, H. M., Rule, G. S., Tomasello, J. & Whittaker, M. (1987) *Biochemistry* 26, 6058–6064.
7. Balakrishnan, K., Hsu, F. J., Hafeman, D. G. & McConnell, H. M. (1982) *Biochim. Biophys. Acta* 721, 30–38.
8. Chirgwin, J. M., Przybyla, A. E., MacDonald, R. J. & Rutter, W. J. (1979) *Biochemistry* 18, 5294–5299.
9. Feinberg, A. & Vogelstein, B. (1983) *Anal. Biochem.* 132, 6–13.
10. Sanger, F., Nicklen, S. & Coulson, A. R. (1977) *Proc. Natl. Acad. Sci. USA* 74, 5463–5468.
11. Biggin, M. D., Gibson, T. J. & Hong, G. F. (1983) *Proc. Natl. Acad. Sci. USA* 80, 3963–3965.
12. Kabat, E. A., Wu, T. T., Reid-Miller, M., Perry, H. M. & Gottesman, K. S. (1987) *Sequences of Proteins of Immunological Interest* (Natl. Inst. of Health, Bethesda, MD).
13. Bilofsky, H. S., Burks, C., Fickett, J. W., Good, W. B., Lewitter, F. I., Rindone, W. P., Swindell, C. D. & Tung, C. S. (1986) *Nucleic Acids Res.* 14, 1–4.
14. Mount, S. M. (1982) *Nucleic Acids Res.* 10, 459–472.
15. Golding, G. B., Gearhart, P. J. & Glickman, B. W. (1987) *Genetics* 115, 169–176.
16. Jardetzky, O. & Roberts, G. C. K. (1981) *NMR in Molecular Biology* (Academic, New York).
17. Linse, S., Brodin, P., Drakenberg, T., Thulin, E., Sellers, P., Elmden, K., Grundstrom, T. & Forsen, S. (1987) *Biochemistry* 26, 6723–6735.

Crystallization of the Fab Fragment of a Monoclonal Anti-Spin-Label Antibody With and Without Bound Hapten

Daniel J. Leahy*, Thomas Hynes**, Robert O. Fox**,

and Harden M. McConnell*

*Stauffer Laboratory for Physical Chemistry, Stanford University

Stanford, California 94305

**Dept. of Molecular Biochemistry and Biophysics, Yale University

New Haven, Connecticut 06520

ABSTRACT

The F_{ab} fragment of a monoclonal antibody, AN02, specific for a spin-labelled dinitrophenyl hapten was crystallized both with and without bound hapten. Both crystals formed in phosphate buffered saline (150mM NaCl, 10mM Na_2PO_4, .02% NaN_3, pH 7.4) at 4°C and diffract to at least 2.2 Å resolution. F_{ab} with bound hapten crystallizes in space group $P6_122$ or $P6_522$ with cell dimensions a=b=73 Å and c=373 Å. Unoccupied F_{ab} also crystallizes in space group $P6_122$ or $P6_522$ but with cell dimensions a=b=75 Å and c=376 Å.

The structural change that an antibody undergoes upon binding of antigen is interesting in terms of antibody diversity and function. Independent crystal structures of an antibody both with and without antigen have not yet been solved. We report here the crystallization of the F_{ab} fragment of AN02, a monoclonal antibody specific for a spin-labelled dinitrophenyl hapten, with and without hapten (for the chemical structure of this hapten see Anglister et al. (1984a)).

In addition to allowing assessment of the effect of hapten binding on antibody structure, solution of the AN02 crystal structures will enable a comparison of x-ray and NMR structural information. The bound spin-label hapten broadens NMR signals of nearby ($<17\text{Å}$) protons in a strongly distance dependent manner. An NMR difference spectrum, F_{ab} alone minus F_{ab} with bound spin-label, is dominated by resonances from protons near the electron spin. Culturing the antibody producing cells in media containing specific deuterated amino acids results in virtually complete incorporation of the deuterated amino acids into the antibody. The spin-label's broadening effect, in combination with deuteration, has enabled identification of NMR signals from amino acids in the hapten binding site and measurement of the distance between many of these residues and the electron spin (Anglister et al., 1984a;1984b;1987).

The genes coding for the AN02 heavy and light chains have recently been cloned (Leahy et al., 1988), and a panel of AN02 mutants is currently being constructed using site directed mutagenesis. The ability to use NMR, x-ray, and recombinant DNA techniques makes AN02 and its mutants a rich source for study of structural and functional aspects of the antibody combining site.

The F_{ab} fragment was prepared as described previously for NMR studies (Anglister et al., 1984a). Briefly, whole antibody was isolated from tissue culture supernatants with a protein A-sepharose column. The antibody was concentrated by vacuum dialysis and digested with papain. The F_{ab} fragment was separated from the F_c fragment and smaller digestion products by chromatography on a G-75 sephadex column followed by a protein A-sepharose column. The product was concentrated to 20 mg/ml and dialysed into phosphate buffered saline (150mM NaCl, 10mM Na_2PO_4, .02% NaN_3, pH 7.4). To prepare samples of

F_{ab} with hapten, an excess of solid hapten was added to the F_{ab} and the mixture gently rotated at room temperature for four hours. The sample was then spun in a microfuge at 15,000 rpm for 20 min and the hapten saturated F_{ab} supernatant removed. From UV absorption spectra we estimate that less than .01% of the F_{ab} in these samples is free of hapten. The F_{ab} samples were centrifuged a second time for 20 min at 15,000 rpm in a microfuge, and the solution aliquotted into 5 mm glass NMR tubes. The samples were then maintained at 4°C.

Crystals formed after approximately two weeks with different tubes containing different sized crystals. Most crystals grew as hexagonal barrels with the longest dimension along the six-fold axis. Either many small crystals coated the NMR tubes and did not appear to grow significantly after first observation, or a few crystals appeared which then continued to grow to a much larger size. In cases where a few large crystals appeared, crystals grew to an average size of 0.5x0.5x0.7mm. One crystal grew to approximately 2x2x3mm.

Crystals were mounted in quartz capillaries and screened precession photographs (μ=15°) of the hk0, h0l, and 111 planes were taken using rotating anode radiation. Crystals of AN02 F_{ab} both with and without hapten crystallized in space group $P6_1 22$ or $P6_5 22$. The cell dimensions for F_{ab} alone are a=b=75 Å and c=376Å, and the cell dimensions for F_{ab} with the spin-label hapten bound are a=b=73Å and c=373 Å. Both crystals withstand x-rays well and diffract to greater than 2.2 Å resolution, making them suitable for x-ray crystallographic studies.

Acknowledgements

REFERENCES

Anglister, J., Frey, T., & McConnell, H. M. (1984a) Biochemistry 23, 1138-1142.

Anglister, J., Frey, T., & McConnell, H. M. (1984b) Biochemistry 23, 5372-5375.

Anglister, J., Bond, M. W., Frey, T., Leahy, D. J., Levitt, M., McConnell, H. M., Rule, G. S., Tomasello, J., & Whittaker, M. (1987) Biochemistry 26, 6058-6064.

Leahy, D. J., Rule, G. S., Whittaker, M., & McConnell, H. M. (1988) Biochemistry, to be published.

SPECIFICITIES OF GERM LINE ANTIBODIES

Thomas P. Theriault, Gordon S. Rule and Harden M. McConnell

Stauffer Laboratory for Physical Chemistry
Department of Chemistry
Stanford University
Stanford, California 94305, USA

The past few years have seen remarkable progress in research on the structure and function of antibodies. In our own work we have shown that it is possible to obtain extensive significant information on the composition and structure of antibody combining sites using NMR, together with nitroxide spin-label haptens (Anglister et.al., 1984a, 1985 and 1987; Frey et .al., 1984). This derived information includes the amino acid composition of the combining site region, that is, the number of tyrosines, alanines, etc. that are within ~ 20 Å of the odd electron on the paramagnetic hapten. In antibody molecules there are typically 40-50 amino acids in this combining site region. We have shown that NMR titration data can be used to estimate distances between individual protons on amino acid side chains and the odd electron (Anglister et.al., 1984b; Frey et. al., 1988). These measured distances extend out to about 20 Å, and in to distances of the order of 3-5 Å. Shorter distances can sometimes be estimated from nuclear magnetization transfer experiments. The NMR data also provide a powerful and convenient means of obtaining the on-off kinetics of hapten-antibody reactions, using resonance signals from the hapten as well as from the protein.

Our NMR studies are being carried out on 12 monoclonal anti-dinitrophenyl nitroxide spin label antibodies that we have prepared and sequenced (cDNA) (Leahy et.al., 1988). Theoretical models for the Fab fragments of all of these antibodies have been made in collaboration with Dr. Michael Levitt (unpublished). A major purpose of our current work is to compare these theoretical structure models and the NMR data. An essential requirement for this work is the production of antibody mutants that can be used to obtain rigorous NMR assignments.

Figures 1 and 2 show schematically the sequence similarities of the Fab fragments of the antibodies AN01-AN12. Some pairs of these antibodies have

sequences that are very similar in both heavy and light chains (AN01,2,3), or (AN05,6), some pairs have similarities in only the heavy chains (AN04,11,12), and other pairs have similarities in only the light chains (AN07-AN10). Clearly many sequences can accommodate the same hapten. Since germline antibody genes doubtless evolved long before dinitro-phenyl was first synthesized, we have developed an interest in the question of whether the germline antibodies would also recognize the dinitrophenyl nitroxide spin label hapten. If the germline antibodies did not recognize this hapten, then we would conclude that their specificity/affinity was largely developed through somatic mutation. If the germline antibodies did recognize the dinitrophenyl nitroxide spin label hapten with essentially the same specificity/affinity, then we would conclude that the specificity of these antibodies was essentially accidental, and we might then speculate on the nature of the primordial antigen and how its structure might be related to dinitrophenyl.

MATERIALS AND METHODS

Southern Blot Analysis

Balb-c genomic DNA was isolated from the livers of Balb-c mice as described in Maniatis et. al. (1982). AN02 genomic DNA was similarly isolated from AN02 antibody producing hybridoma cells. Each of these DNAs were digested with a series of restriction enzymes and analyzed by the method of Southern (1975). The probes used in the hybridization were prepared from the variable regions of the light and heavy chain coding sequences of an AN02 containing plasmid. The light chain probe was a 1000 base pair fragment made by digesting the AN02 genomic kappa chain clone with BglII and PpuMI. This probe begins approximately 800bp 5' to the variable region. The heavy chain probe was a 600bp fragment isolated as an XbaI and EcoRI fragment from an AN02 heavy chain clone which extends to within 40 base pairs of the end of the variable region. The probes were labelled using Pharmacia's oligo labelling kit with a-32P dCTP(New England Nuclear) as label. The hybridizations were carried out as described in Maniatis (1982) at 42 degrees Celsius with formamide concentrations ranging from 35% to 50%.

Germline gene cloning and sequencing

Balb-c liver DNA was digested with the appropriate restriction enzyme, size selected on an agarose gel and isolated using an International Biotechnology Unidirectional Electroelutor. Libraries were made by ligating these fragments into either lambda ZAP or lambda NM590. Recombinant phage DNA was packaged as described in Maniatis (1982) and the resultant libraries were screened using either the heavy or light chain probe. Positive clones were purified and subcloned into pUC322 from lambda NM590 or excised from lambda ZAP into its pBluescript phagemid. The plasmid clones were mapped with 15 to 35 combinations of single and double restriction digests. The clones were subcloned again into M13 vectors and sequenced by the dideoxy method with a-35S dATP as label. (New England Nuclear)

RESULTS

Rearrangement of Balb-c DNA

Genetic rearrangement as indicated by restriction fragment length polymorphism is evidenced by the results of the Southern blot experiments shown in figures 3 and 4. In the case of the heavy chain for AN02, the DNA sequence of the variable region was known to share 97.6% sequence identity with a heavy chain Balb-c germline sequence named SB32 and with the variable region of a gene isolated from an IgM producing hybridoma LB8 published by Dzierzak et.al. (1986). The hybridization of fragments obtained by digestion with the enzymes EcoRI, HindIII, and XbaI shows a pattern consistent with what had been seen previously, namely hybridization to a 2.4 kb EcoRI fragment, an 7.5 kb HindIII fragment, and a 7.0 kb XbaI fragment. The AN02 genomic heavy chain gene is known to be contained on a 4.6 kb EcoRI and a 1.9 kb XbaI fragment (G. Rule unpublished data). These fragments are seen to hybridize as would be expected. Our assumption then was that a Balb-c germline variable region gene which was contained on 2.4 kb EcoRI and 7.0 kb XbaI fragments was rearranged by the processes of recombination and somatic mutation such that it rested on 4.6 kb EcoRI and 1.9 kb XbaI

4

fragments in the AN02 genome. The results for digestion with HindIII are less clear, since the size of the restriction fragment which contains the AN02 genomic heavy chain gene is not known. The patterns seen in the double digestion with XbaI/HindIII and XbaI/KpnI, indicate that the single band in the XbaI lane results from more than one germline variable region.

In the case of the light chain a large number of fragments cross hybridize with the AN02 light chain probe indicating that the AN02 kappa variable gene comes from a large family of related germline genes. Most of the hybridizing bands seen in the Balb-c lanes are matched by equivalent bands in AN02. The major difference is that a 3.7 kb HindIII fragment hybridizes with approximately twice as much intensity in Balb-c as in AN02. This pattern would be expected if only one of the allelic light chain containing chromosomes were recombined during the differentiation of the AN02 producing B lymphocyte and if the rearranged germline variable gene were situated at the 3' end of the family of cross reacting variable regions. Further evidence that the AN02 light chain germline is contained on a 3.7 kb HindIII fragment comes from performing the hybridization under more stringent conditions. Only the bands at 3.5, 3.7, and 3.9 kb appear, and the 3.7 kb band is the most intense.

Cloning and sequencing of germline genes

To determine whether the SB32 gene was indeed the germline gene for AN02 or if a gene with even more sequence identity exists, the 7.0 kb XbaI as well as the 7.5 kb HindIII fragments were ligated into lambda ZAP and lambda NM590 respectively. Multiple positive clones were purified and sequenced from both libraries and in each case a germline gene was obtained with greater than 99% sequence identity to the heavy chain variable region of the antibody AN07 and only 92% sequence identity to AN02. Since the antibody AN07 has a lambda type light chain, the complete germline configuration of AN07 could be deduced. The inability to find the SB32 germline gene or any other AN02-like gene in the XbaI or HindIII libraries upon sequencing 14 independent clones indicated that there may have been a systematic problem with the vectors or hosts used in the cloning process. To better understand the clonability of these variable genes, as well as to obtain partial sequence data for other germline

variable regions, a library was constructed which contained EcoRI/XbaI Balb-c DNA fragments of approximately 600 base pairs in length. Two AN02-like germline genes were sequenced from this library in the five clones which have been purified. One of these was the SB32 germline, the other was a gene that was only 87% similar to AN02.

For the light chain germline gene libraries were made in lambda NM590 with HindIII fragments of approximately 3.5, 3.7, and 3.9 kb. Positive clones were purified and sequenced in each case. Two light chain germline genes were found on the 3.5 kb fragments which were 94% similar to the AN02 light chain, one was found on the 3.9 kb fragment that was 96% similar, and one was found on the 3.7 kb fragment which had more than 98% sequence identity. This is assumed to be the germline gene for the light chain variable region of AN02.

Construction of antibody genes in the recombined germline state.

In order to investigate the binding properties of the IgM class antibody which was found on the surface of the lymphocyte clone that eventually mutated into AN02 or AN07, it is necessary to first make genetic constructs which reflect the sequence of this germline antibody and then express these constructs in a suitable system. Taking the variable regions described above as the true germline variable genes, the remainder of the recombined antibody genes can be found in the germline joining and diversity sequences which have been well characterized (Kabat et. al. 1987). For AN07 the diversity segment DFL16.1 and the joining segments JH3 and JL1 were used. For AN02 the diversity segment was too short to determine unambiguously while the joining segments JH3 and JK5 were used. The inferred protein sequence of the heavy and light chain cDNA clones for AN02 and AN07 together with that of the corresponding germline variable regions, diversity segments and joining regions recombined in the proper reading frame are shown in figures 5 and 6. In each case more than 97% of the protein residues for each antibody can be assigned to their germline states. The ambiguities that exist occur at the junctions between the variable regions, joining, and diversity segments. At splice junctions it is impossible to determine which germline splice partner donated the germline sequence since mutation after recombination could

6

convert one sequence into the other. Compounding this problem in the heavy chains is the mechanism of nucleotide insertion which can place random nucleotides into the V-D and D-J junctions during recombination. However, given that the observed mutation rate in antibody genes during somatic diversification is approximately 0.5% (Gearhart et. al. 1983), the small set of ambiguous nucleotides is highly likely to have been the same in the germline as in the mature antibody gene. In the worst case, AN02 with 11 ambiguous nucleotides, the probability is still approximately 95% that the inferred protein sequence for all of these codons correctly represent the germline.

Future studies.

Site specific mutatgenesis has already been used to change the AN02 light chain cDNA clone into the germline gene sequence defined above. Progress is currently underway to construct the other germline genes from the cDNA clones by either site directed mutagenesis or where suitable restriction sites exist, by replacement with the germline DNA itself. These constructs will then be used in an expression system from which mutant protein can be obtained. Studies will then center on characterizing these proteins in terms of their binding affinities and kinetics for various DNP derivatives.

DISCUSSION

The results of the germline sequencing for AN07 indicate that very little somatic mutation occurred for this antibody. Only two residue changes exist between the known germline genes and the cDNA clones. One of these is removed from the complementary determining regions and is not considered to be a factor. The other occurs in CDR 1 of the light chain. Modelling studies suggest that this residue is removed from the binding pocket and will not be in contact with the bound hapten. Thus we expect the germline antibody and AN07 to have the same affinity for the DNP haptens.

The AN02 germline has a total of 11 residue differences from the sequence of AN02, however only 3 of these occur in the hypervariable loops. Although two of these occur in residues of the second hypervariable loop of the heavy

7

chain they are well removed from our model of the binding pocket and are unlikely to have any significant effect on the binding of the hapten. The residue change in CDR 2 of the light chain, Ser in the germline to Tyr in AN02 at position 31, can also be considered unimportant since NMR studies of tyrosines have implicated only one tyrosine, Tyr34L, as being in contact with the hapten (Rule et.al., in preparation). We believe that the antibody in its germline state will have a similar affinity and show similar kinetics to the mature antibody as far as the DNP haptens are concerned.

The plausible assumption that the germline antibodies bind DNP haptens leads us to the conclusion that the DNP specificities of these antibodies are essentially accidental since the germline genes could have only experienced evolutionary pressure in response to naturally occurring antigens. The question then arises as to what the primordial antigen might have been. For example, on the molecular scale, was it big or small? Our NMR studies of the antibodies AN01, AN02, and AN03 show a remarkably large concentration of aromatic residues, especially tyrosines, in the combining site region. In our most studied molecule, AN02, there are 8-10 tyrosine residues in this region (Anglister et. al., 1984), many more than could possibly all be in contact with the hapten. Further, as will be discussed elsewhere (Rule et. al., in preparation), the sharp proton resonance signals from these residues, with one notable exception, show almost no change on hapten binding, leading us to believe they play no functional role in the binding of DNP haptens. Kinetics studies of antibody-hapten binding also support the view that no significant change in protein structure takes place on hapten binding. We therefore suggest that the primordial antigen recognized by these germline genes was large, with a size of the order of a protein antigen. Studies of other antibody-protein complexes (Amit et. al., 1986; Sheriff et. al., 1987) typically show that the antibody recognition area is large, on the order of 700 square angstroms of interface. Furthermore, AN02 has been shown to be a cryoglobulin (Theriault et. al., in preparation), indicating a possible role for the binding site aromatic residues in idiotype-antiidiotype regulation, the idiotype here being self protein. These ideas will be developed in fuller detail elsewhere.

ACKNOWLEDGEMENTS

REFERENCES

Amit, A. G., Mariuzza, R. A., Phillips, E. V. and Poljak. R. J., 1986, Three-dimentional structure of an antigen-antibody complex at 2.8 A resolution, Science, 233:747.

Anglister, J., Frey, T. and McConnell, H. M., 1984, Magnetic resonance of a monoclonal anti-spin-label antibody, Biochemistry, 23:1138.

Anglister, J., Frey, T. and McConnell, H. M., 1984, Distances of tyrosine residues from a spin-label hapten in the combining site of a specific monoclonal antibody, Biochemistry, 23:5372.

Anglister, J., Bond, B. W., Frey, T, Leahy, D. J., Levitt, M., McConnell, H. M., Rule, G. S., Tomasello, J. and Whittaker, M. M., 1987, Contribution of tryptophan residues to the combining site of a monoclonal anti-dinitrophenyl spin-label antibody, Biochemistry, 26:6058.

Anglister, J., Frey, T. and McConnell, H. M., 1985, NMR technique for assessing contributions of heavy and light chains to an antibody combining site, Nature, 315.6014:65.

Dzierzak, E. A., Janeway, C. A.,Jr., Richard, N. and Bothwell, A., 1986, Molecular characterization of antibodies bearing Id-460, J. Immunol., 136.5:1864.

Frey, T., Anglister, J. and McConnell, H. M., 1984, Nonaromatic amino acids in the combining site of a monoclonal anti-spin-label antibody, Biochemistry, 23:6470.

Frey, T., Anglister, J. and McConnell, H. M., 1988, Line-shape analysis of NMR difference spectra of an anti-spin-label antibody, Biochemistry, 27:5161.

Gearhart, P. J. and Brogenhagen, D. F., 1983, Clusters of point mutations are found exclusively around rearranged antibody variable genes, Proc. Natl. Acad. Sci. USA, 80:3439.

Leahy, D. J., Rule, G. S., Whittaker, M. M. and McConnell, H. M., 1988, Sequences of 12 monoclonal anti-dinitrophenyl spin-label antibodies for NMR studies, Proc. Natl. Acad. Sci. USA, 85:3661.

Kabat, E. A., Wu, T. T., Reid-Miller, M., Perry, H. M. and Gottesman, K. S., 1987, "Sequences of Proteins of Immunological Interest", Natl. Inst. of Health, Bethesda, MD.

Maniatis, T., Fritsch, E. F. and Sambrook, J., 1982, "Molecular Cloning : A Laboratory Manual", Cold Spring Harbor Laboratory, Cold Spring Harbor.

Sheriff, S., Silverton, E. W., Padlan, E. A., Cohen, G. H., Smith-Gill, S. J., Finzel, B. C. and Davies, D. R., 1987, Three-dimensional structure of an antibody-antigen complex, Proc. Natl. Acad. Sci. USA, 84:8075.

Southern, E., 1975, Detection of specific sequences among DNA fragments separated by gel electrophoresis, J. Mol. Biol., 98:503.

```
                    -20        -10         1          10         20    27

                     |          |          |          |          |     ABC

ANO2         MDFQVQIFSFLLISASVILSRGQIVLTQSPAIMSASPGEKVTMTCSASS
ANO1         ............M.....M............L................
ANO3         ........M.....M............L................
ANO9         ..............I..VM...EN.........I...L......S.R...
ANO5            MRCSLQFLGVLMFWISGVS.D..I..DELSNPVAS..S.SIS.RSTKSLL
ANO6            MRCSLQFLGVLMFWISGVS.D..I..DELSNPVTS..S.SIS.RSTKSLL
ANO4            MR.LAELLG.LLFCFLGV.CD.QMN...SSL...L.DTI.I..H..Q
ANO8            MRF.VQVLG.LLLWISGAQCDVQI....SYLA.....TIIIN.R..K
AN11            MVFTPQILG.MLFWISA...D........TL.VT..DS.SLS.R..Q
AN12         MHHTSMGIKMES..QV.VFVFLWLSGVD.D..M...HKF..T.V.DR.SI..K..Q
ANO7            MAW.SLI.SLL.LSSGAIS.A.V..ES. LTT....T..L..RS.N
AN1O            MAW.SLI.SLL.LSSGAIS.A.V..ES. LTT....T..L..RS.T

                 30         40         50         60         70         80

           DEF   |          |          |          |          |          |

ANO2         SVYYMYWYQQKPGSSPRLLIYDTSNLASGVPVRFSGSGSGTSYSLTISRMEAEDAA
ANO1         ..S..F......R...KPW..L.........A...............S.......
ANO3         ..S..F......R...KPW.FL.........A....R............S.......
ANO9         ..N..F.....SDA..K.W..Y.....P...A........N.......S.AG....
ANO5         YK DGKT.LN.FL.R..Q..Q....LM.TR....SD........DFT.E...VK...VG
ANO6         YK DGKT.LN.FL.R..Q..Q....LM.TR....SD........DFT.E...VK...VG
ANO4            NINVWLS.......NI.K....KA...HT...S.........FT....SLQP..I.
ANO8            SISK.LA...E...KTNK....SG.T.Q..I.S........DFT....SL.P..F.
AN11            SVSNNLH.F...SHE......KYA.QSI..I.S........DFT.S.NSV.T..FG
AN12            DVSTAVA.......Q..K....SA.YRYT...D..T......DFTF...SVQ...L.
ANO7         GAVTTSN.AN.V.E..DHLFTG..GG.N.R.P...A.....LI.DKAA...TGAQT..E.
AN1O         GAVT.SNSVK.V.E..DHLFTG..GGSN.R.P...A.....LI.DKAA...AGAQT..E.

                 90    95         100    106 109

                  |    ABCDEF      |      A  |

ANO2         TYYCQQWSSYPP       ITFGVGTKLEL KRA
ANO1         .........N..       ....S.....I ...
ANO3         .......N.I..       ....A...... ...
ANO9         ......FT.S.        S...A...... ...
ANO5         V.....LVEF.        L...A...... ...
ANO6         V.....LVEF.        L...A...... ...
ANO4         ......GQ...        L.L.G.....I ...
ANO8         M.....HNE..        Y...G.....I ...
AN11         M.F...SN.W.        F...G.....I ...
AN12         V...H.HY.S.        Y...G.....I ...
ANO7         I.F.AL.Y.NH        LV..G....TVLGQP
AN1O         V.F.AL.Y.NH        LV..G.A..TVLGQP
```

Figure 1. Deduced amino acid sequences of the V regions of the light chains of the anti-DNP-SL monoclonal antibodies AN01-AN12. Numbering system according to Kabat et.al. (1987). From Leahy et.al. (1988).
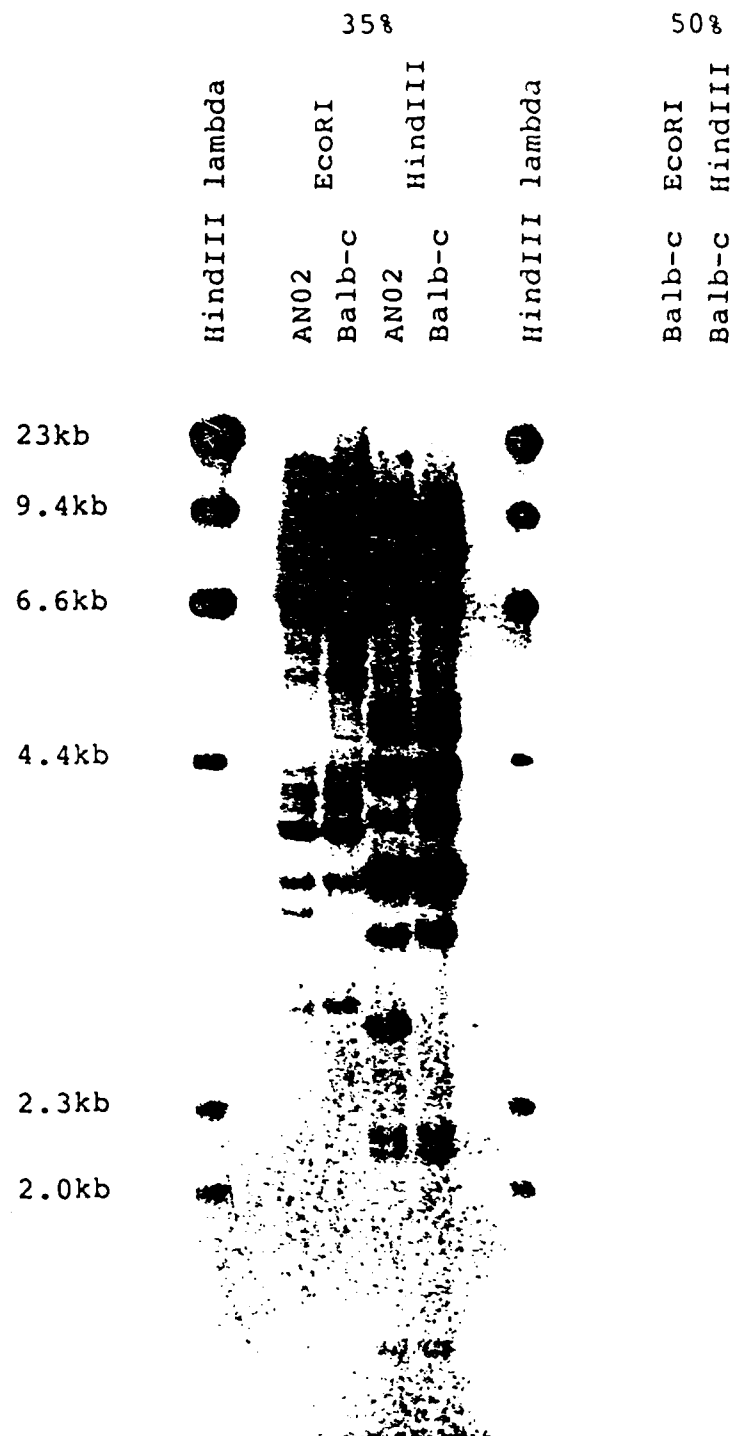
Figure 3. Southern blot results using the light chain probe.
AN02 hybridoma and Balb-c genomic DNA were digested with
HindIII and EcoRI. Fragment sizes were internally
referenced by including HindIII digested lambda DNA in the
gel and as a radiolabelled probe. Shown are experiments in
whicn the hybridizations were carried out in 50% and 35%
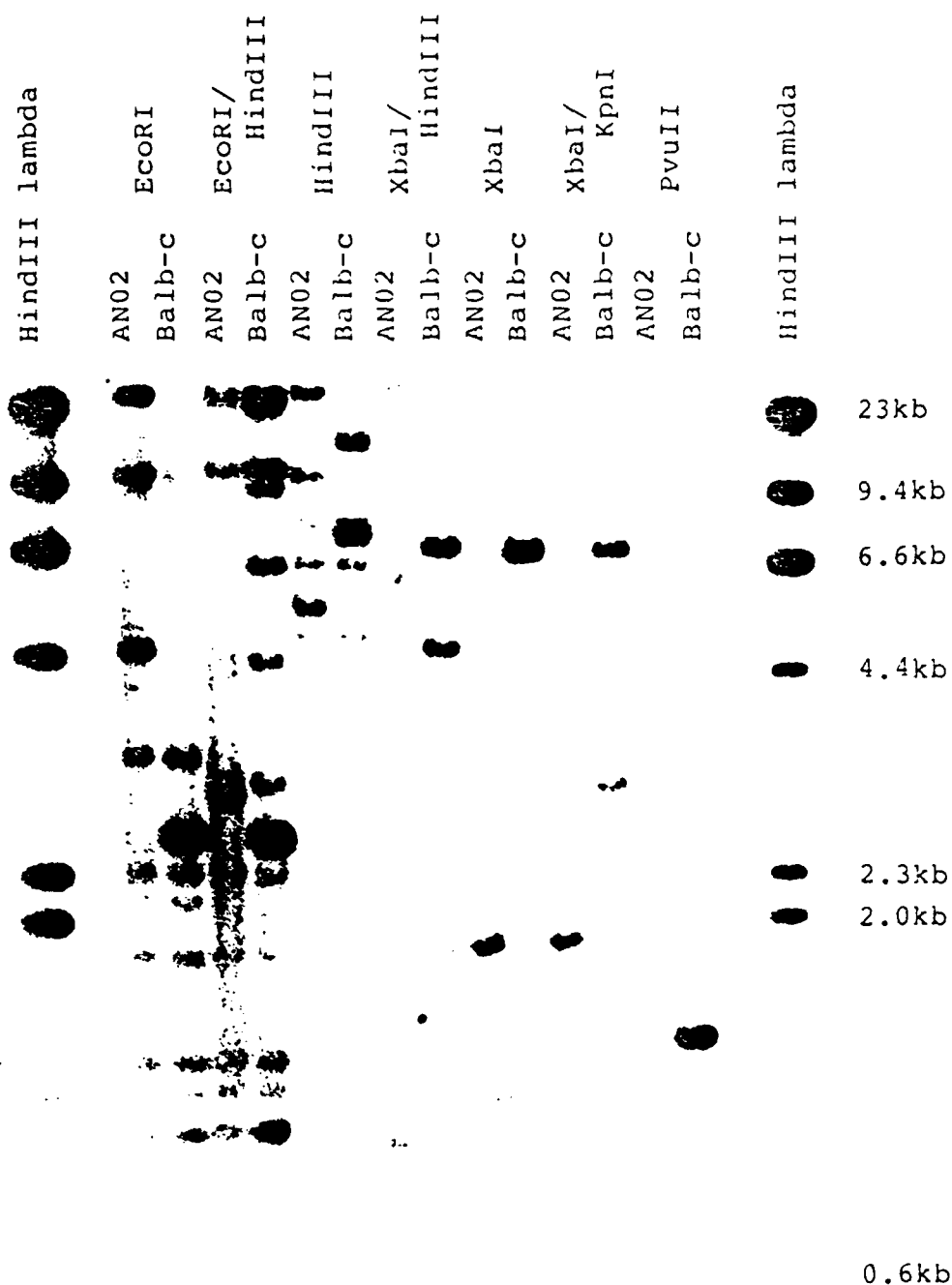formamide.

Figure 4. Southern blot results using the heavy chain probe. AN02 hybridoma and Balb-c genomic DNA were digested with the same enzymes. Fragment sizes were internally referenced by including HindIII digested lambda DNA in the gel and as a radiolabelled probe.